Both p16^{Ink4a} and the p19^{Arf}-p53 pathway constrain progression of pancreatic adenocarcinoma in the mouse

Nabeel Bardeesy[a,b,c], Andrew J. Aguirre[a,c], Gerald C. Chu[a,d,e], Kuang-hung Cheng[b], Lyle V. Lopez[a], Aram F. Hezel[a], Bin Feng[a,e], Cameron Brennan[f], Ralph Weissleder[g], Umar Mahmood[g], Douglas Hanahan[h], Mark S. Redston[d], Lynda Chin[a,e,i], and Ronald A. DePinho[a,e,j,k,l]

[a]Department of Medical Oncology and [e]Center for Applied Cancer Science, Dana–Farber Cancer Institute, Harvard Medical School, Boston, MA 02115; [j]Departments of Medicine and [d]Pathology, Brigham and Women's Hospital, Harvard Medical School, Boston, MA 02115; [k]Department of Genetics and [i]Departments of Dermatology and of Biological Chemistry and Molecular Pharmacology, Harvard Medical School, Boston, MA 02115; [b]Massachusetts General Hospital Cancer Center and [g]Center for Molecular Imaging Research, Massachusetts General Hospital, Harvard Medical School, Boston, MA 02114; [f]Neurosurgery Service, Memorial Sloan–Kettering Cancer Center, New York, NY 10021; and [h]Department of Biochemistry, Diabetes Center and Comprehensive Cancer Center, University of California, San Francisco, CA 94143

Communicated by David M. Livingston, Dana–Farber Cancer Institute, Boston, MA, February 16, 2006 (received for review November 19, 2005)

Activating *KRAS* mutations and *p16^{Ink4a}* inactivation are near universal events in human pancreatic ductal adenocarcinoma (PDAC). In mouse models, Kras^{G12D} initiates formation of premalignant pancreatic ductal lesions, and loss of either *Ink4a*/*Arf* (*p16^{Ink4a}*/*p19^{Arf}*) or *p53* enables their malignant progression. As recent mouse modeling studies have suggested a less prominent role for *p16^{Ink4a}* in constraining malignant progression, we sought to assess the pathological and genomic impact of inactivation of p16^{Ink4a}, p19^{Arf}, and/or p53 in the Kras^{G12D} model. Rapidly progressive PDAC was observed in the setting of homozygous deletion of either *p53* or *p16^{Ink4a}*, the latter with intact germ-line p53 and *p19^{Arf}* sequences. Additionally, Kras^{G12D} in the context of heterozygosity either for *p53* plus *p16^{Ink4a}* or for *p16^{Ink4a}*/*p19^{Arf}* produced PDAC with longer latency and greater propensity for distant metastases relative to mice with homozygous deletion of *p53* or *p16^{Ink4a}*/*p19^{Arf}*. Tumors from the double-heterozygous cohorts showed frequent p16^{Ink4a} inactivation and loss of either p53 or p19^{Arf}. Different genotypes were associated with specific histopathologic characteristics, most notably a trend toward less differentiated features in the homozygous *p16^{Ink4a}*/*p19^{Arf}* mutant model. High-resolution genomic analysis revealed that the tumor suppressor genotype influenced the specific genomic patterns of these tumors and showed overlap in regional chromosomal alterations between murine and human PDAC. Collectively, our results establish that disruptions of p16^{Ink4a} and the p19^{ARF}-p53 circuit play critical and cooperative roles in PDAC progression, with specific tumor suppressor genotypes provocatively influencing the tumor biological phenotypes and genomic profiles of the resultant tumors.

array comparative genomic hybridization | mouse models | pancreatic cancer | KRAS | tumor suppressor

Pancreatic ductal adenocarcinoma (PDAC) ranks as the fourth leading cause of cancer mortality in the United States and causes >200,000 deaths worldwide annually (1, 2). Histopathological analyses have identified precursor lesions, pancreatic intraepithelial neoplasias (PanIN), which appear to progress through increasingly severe stages of cellular atypia leading to invasive PDAC (3). These lesions show multistep molecular progression that includes early activating *KRAS* mutations and telomere attrition, and subsequent inactivation of *p16^{Ink4a}*, *p14^{ARF}*, *p53*, and/or *SMAD4* tumor suppressors in a high percentage of cases (4–6).

The *Ink4a*/*Arf* locus (hereafter denoted *p16^{Ink4a}*/*p19^{Arf}*) encodes tumor suppressors *p16^{INK4A}* and *p14^{ARF}* (*p19^{Arf}* in the mouse). p16^{INK4A} is a G_1 cyclin-dependent kinase (CDK) inhibitor that binds to CDK4 and CDK6 and prevents their association with D-type cyclins (7), thereby facilitating CDK4/6-cyclin D-mediated phosphorylation and inactivation of retinoblastoma protein (RB) and S-phase entry. p16^{INK4A}-mediated tumor suppression may relate to its induction by activated oncogenes and consequent promotion of oncogene-induced senescence (8, 9). *p14^{ARF}* inhibits MDM2-mediated degradation of p53 (10, 11); thus, loss of p14^{ARF} results in reduced p53 protein levels (12). Mounting evidence suggests that p14^{ARF} also possesses p53-independent functions including the inhibition of ribosomal RNA processing (13, 14).

The central role of *p16^{INK4A}* in PDAC is evidenced by its inactivation in 80–95% of sporadic cases (15) and by increased PDAC risk associated with germ-line *p16^{INK4A}* mutations (16, 17). Whereas mutations exclusively targeting *p16^{INK4A}* and sparing *p14^{ARF}* have been identified in human PDAC, *p14^{ARF}*-specific mutations have not been reported. However, the pathogenetic relevance of p14^{ARF} is suggested by the occurrence of homozygous *p16^{INK4A}*/*p14^{ARF}* deletions in a subset of PanIN lesions, as well as in ≈40% of PDAC (6, 18). An important unresolved issue is the extent to which this correlation reflects the functional benefits of eliminating both *p16^{INK4A}* and *p14^{ARF}*, or rather a bystander phenomenon whereby *p14^{ARF}* loss occurs as a consequence of targeting the overlapping *p16^{Ink4a}* coding sequences.

p53 regulates target genes governing diverse tumor suppressor processes (19). *p53* is mutated in 50–75% of human PDAC coupled with loss of the remaining WT allele (6). These mutations typically occur in advanced PanIN lesions that have previously incurred KRAS activation and p16^{INK4A} loss (20, 21). *p53* mutations and *p14^{ARF}* deletions coexist in ≈38% of human PDAC cases (6, 18, 20, 22). Although such data may imply nonoverlapping tumor suppressor roles for these proteins, the distinct requirements for p53 vs. p14^{ARF} inactivation in PDAC development have not been explored by genetic means.

The frequency and temporal occurrence of mutations in *KRAS*, *p16^{INK4A}*/*p19^{ARF}* and *p53* in human PanIN and PDAC support the view that activated KRAS cooperates with defects in the RB and p53 tumor suppressor pathways to drive the initiation and progression of the disease. This hypothesis has received additional support from genetically engineered mouse models of PDAC. Endogenous Kras^{G12D} expression in the mouse pancreas promotes development of PanINs (23, 24) that can progress to PDAC after a long latency (23). Furthermore, pancreas-specific expression of Kras^{G12D} in the

Conflict of interest statement: No conflicts declared.

Abbreviations: PDAC, pancreatic ductal adenocarcinoma; PanIN, pancreatic intraepithelial neoplasias; CDK, cyclin-dependent kinase; RB, retinoblastoma protein; aCGH, array-comparative genomic hybridization; CNAs, copy number alterations.

[c]N.B. and A.J.A. contributed equally to this work.

[l]To whom correspondence should be addressed. E-mail: ron_depinho@dfci.harvard.edu.

Table 1. PDAC Incidence, Latency, and Histological Phenotype

Genotype	No. of tumors	Average latency, weeks	Metastasis, %	Histology			aCGH‡	
				Adenocarcinoma	Sarcomatoid	Anaplastic	Kras	Myc
$p16/p19^{lox/lox}$	27	8.5	11	48* (81)†	26 (37)	26 (70)	13/16	1/16
$p16/p19^{lox/+}$	12	34.2	69	57 (57)	43 (43)	0 (0)	5/8	1/8
$p53^{lox/lox};p16^{+/+}$	3	6.2	0	100 (100)	0 (33)	0 (33)	1/3	0/3
$p53^{lox/lox};p16^{+/-}$	5	6.5	0	80 (100)	0 (0)	20 (100)	3/4	3/4
$p53^{lox/lox};p16^{-/-}$	5	7.2	20	40 (80)	0 (0)	60 (100)	0/3	0/3
$p53^{lox/+};p16^{+/+}$	3	21.8	33	100 (100)	0 (33)	0 (33)		
$p53^{lox/+};p16^{+/-}$	16	14.7	25	81 (88)	19 (19)	0 (44)	1/6	2/6
$p53^{lox/+};p16^{-/-}$	4	13.1	25	75 (100)	25 (50)	0 (50)	—	
$p53^{+/+};p16^{-/-}$	3	18.3	33	0 (33)	100 (100)	0 (0)		
$Kras^{G12D}$	3	57	67	0 (33)	100 (100)	0 (0)		

*Percentage of tumors in which the particular histology predominates (see *Materials and Methods*).
†The percentage of tumors in which the particular histology is present in any proportion.
‡Number of tumors with copy number gains of Kras or Myc.

setting of homozygous deficiency at the $p16^{Ink4a}/p19^{Arf}$ locus results in rapid advancement of PanIN to invasive PDAC (24). These observations indicate that activated *Kras* initiates PanIN and $p16^{Ink4a}/p19^{Arf}$-deficiency promotes PanIN-to-PDAC progression. The relative contributions of $p16^{Ink4a}$ and $p19^{Arf}$ to tumorigenesis was not addressed in this model.

A recent model combining $Kras^{G12D}$ and $p53^{R172H}$ alleles produced invasive PDAC, demonstrating that p53 normally functions to suppress the emergence of PDAC (25). Notably, a functional $p16^{Ink4a}/p19^{Arf}$ locus was retained in the $Kras^{G12D}$ $p53^{R172H}$ tumors. Because both p53 and $p16^{INK4A}$ are characteristically lost in human PDAC, these data suggest that there may be cross-species differences in the role of the $p16^{INK4A}$-RB pathway in cellular transformation (26) or, intriguingly, raise the possibility that antecedent loss of p53 function or the gain-of-function properties of the $p53^{R172H}$ protein may serve to neutralize rate-limiting components of the RB pathway. Taken together, the aforementioned studies establish a critical need to genetically examine the cooperative contribution of $p16^{Ink4a}$ inactivation in PDAC progression.

Results

***p53* or *p16Ink4a* Cooperate to Constrain PDAC Progression.** To study the genetic requirements for PDAC progression, we crossed mice with *Pdx1-Cre* (27) and $LSL\text{-}Kras^{G12D}$ alleles (28) and engineered null mutations in *p53* and $p16^{Ink4a}$ or in $p16^{Ink4a}/p19^{Arf}$ (24, 29, 30). Each of these tumor suppressor mutations, alone or in combination, cooperated with $Kras^{G12D}$ activation to promote invasive pancreatic cancers, although with differing tumor latencies and histopathological and genetic properties (Table 1). Hereafter, because all tumors analyzed possess *Pdx1-Cre* and $LSL\text{-}Kras^{G12D}$ alleles, specimens are referred to by their tumor suppressor genotypes. p53 nullizygosity ($p53^{lox/lox}$) caused the most rapid progression, yielding lethal tumors by 8 weeks of age, which is comparable to the latency of homozygous $p16^{Ink4a}/p19^{Arf}$ deletion (23). Notably, in this homozygous-null p53 model, progression kinetics were not appreciably altered by $p16^{Ink4a}$ status (Table 1), suggesting either cross-species differences or that developmental inactivation of p53 may diminish the need for $p16^{Ink4a}$ loss (see below). Thus, it is important to note that $p16^{Ink4a-/-}$ animals, with WT *p53* and $p19^{Arf}$ germ-line status, also developed lethal pancreatic tumors (mean 18.3 weeks).

Because dual inactivation of *p53* and $p16^{Ink4a}$ occurs in most human PDACs, we assessed $Pdx1\text{-}Cre$ $LSL\text{-}Kras^{G12D}$ mice with heterozygous mutations in either or both of these tumor suppressor genes. Tumor latency in $p53^{lox/+}$ $p16^{Ink4a+/-}$ animals was significantly reduced compared with those with $p53^{lox/+}$ alone (see Table 1; 14.7 vs. 21.8 weeks), suggesting cooperative roles for p53 and $p16^{Ink4a}$ in PDAC suppression. Finally, with regard to the relative impact of p53 vs. $p19^{Arf}$ in constraining PDAC progression, we observed that $p16^{Ink4a}/p19^{Arf\,lox/+}$ mice developed PDAC as well, but with longer latency relative to $p53^{lox/+}$ $p16^{Ink4a+/-}$ animals (34.2 vs. 21.8 weeks), suggesting that p53 functions as a more potent barrier to PDAC progression. Overall, the clinical presentation across the various PDAC models was similar and typified by weight loss and jaundice.

Influence of Genotype on Histopathological Presentation. As in other $LSL\text{-}Kras^{G12D}$ models (31), histological analysis revealed that the tumors in this study were carcinomas, predominantly ductal adenocarcinomas, defined by the presence of neoplastic glandular (ductal) cells in a dense fibrous stroma or were alternatively, sarcomatoid or anaplastic carcinoma variants, characterized respectively by spindle-cell morphology or by detached tumor cells with marked nuclear and cytoplasmic pleomorphism, occurring in conjunction with ductal differentiation. The distribution of histological phenotypes was different in the various genetic backgrounds. For example, the proportion of ductal adenocarcinomas was highest in the context of $p53^{lox}$ genotypes (Fig. 1 *A* and *B*). In the $p53^{lox/lox}$ background, $p16^{Ink4a}$ deficiency was associated with a higher frequency of tumors with anaplastic features (Table 1 and Fig. 1*C*). Nevertheless, mice with a $p16^{Ink4a}$ deficiency but WT p53 germ-line status developed ductal adenocarcinomas with regions of sarcomatoid differentiation (Fig. 1 *D–F*). In compound heterozygous mice, ductal adenocarcinomas were more common in the $p53^{lox/+}$ $p16^{Ink4a+/-}$ mice (81% vs. 57% in the $p16^{Ink4a}/p19^{Arf\,lox/+}$ cohort) (Table 1 and Fig. 1 *G* and *J*), whereas sarcomatoid histology was more common in the $p16^{Ink4a}/p19^{Arf\,lox/+}$ tumors (43% compared with 19% in the $p53^{lox/+}$ $p16^{Ink4a+/-}$ tumors) (Table 1 and Fig. 1*L*). Finally, the anaplastic features often observed in tumors from homozygous $p16^{Ink4a}/p19^{Arf\,lox/lox}$ mice (24) were absent in the heterozygous $p16^{Ink4a}/p19^{Arf\,lox/+}$ cohort but were often present focally within ductal adenocarcinomas arising in the $p53^{lox/+}$ $p16^{Ink4a+/-}$ colony (44%)(Table 1 and Fig. 1*I*). Immunohistochemical analysis confirmed the ductal phenotypes of the well differentiated tumors, with positive staining for ductal markers (CK-19 and DBA lectin) and negative for markers of acinar cell (chymotrypsin) or islet cell (insulin) lineages (Fig. 1 *H* and *K* and data not shown). Each model showed invasion and metastasis, although these features were more pronounced in the heterozygous models (Fig. 1 *M–O*). Overall, these results demonstrate significant roles for $p16^{Ink4a}$, $p19^{Arf}$, and *p53* in suppressing pancreatic cancer development and suggest specific impact of mutations in these genes in regulating the differentiation state of the ensuing tumors, most prominently indicating that losses of components of the $p16^{Ink4a}/p19^{Arf}$ locus facilitate the development of more poorly differentiated tumors.

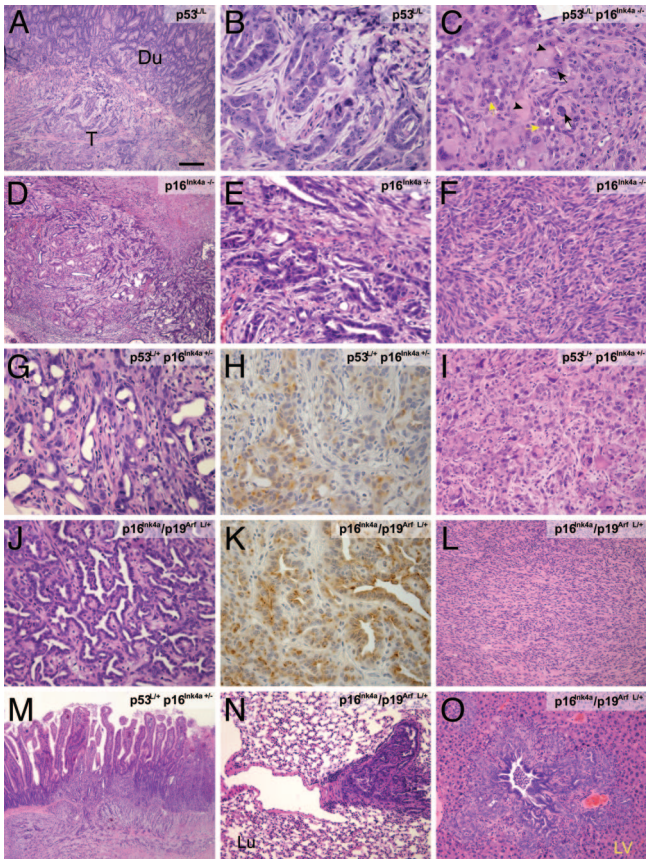

Fig. 1. Deficiency in p53 or p16^{Ink4a} cooperates with oncogenic *Kras*^{G12D} to produce PDAC. (*A*) Hematoxylin/eosin stain of a PDAC (T, tumor) arising in a *p53*$^{lox/lox}$ p16$^{+/+}$ mouse. Note invasion of duodenum (Du). (Scale bar: *A* and *D*, 200 μm; *I*, *N*, and *O*, 100 μm; *B*, *C*, *E–H*, and *J–L*, 50 μm.) (*B*) High-magnification view of the tumor in *A* showing features of ductal adenocarcinoma. (*C*) Tumor from *p53*$^{lox/lox}$ *p16*$^{-/-}$ mouse showing poorly differentiated adenocarcinoma (yellow arrows) admixed with anaplastic epithelioid cells characterized by giant tumor nuclei (black arrows) and eosinophilic inclusions (arrowheads). (*D*) Invasive PDAC arising in *Pdx1-Cre LSL-Kras*^{G12D} *p16*$^{Ink4a-/-}$ mouse. (*E*) High-magnification of *D* showing ductal adenocarcinoma histology. (*F*) Another region of the tumor in *E* showing sarcomatoid differentiation. (*G*) PDAC from *p53*$^{lox/+}$;*p16*$^{Ink4a+/-}$ mouse. (*H*) Positive staining of the tumor in *G* for the ductal marker cytokeratin 19. (*I*) Anaplastic histology in PDAC from the *p53*$^{lox/+}$;p16$^{+/-}$ model. (*J*) Well differentiated *p16*^{Ink4a}/*p19*$^{Arf\ lox/+}$ PDAC. (*K*) Positive staining of tumor in *J* for cytokeratin 19. (*L*) *p16*^{Ink4a}/*p19*$^{Arf\ lox/+}$ tumor showing sarcomatoid histology. (*M*) *p53*$^{lox/+}$*p16*$^{+/-}$ tumor invading the duodenum. (*N* and *O*) *p16*^{Ink4a}/*p19*$^{Arf\ lox/+}$ tumors with metastases to the lung (*N*) and liver (LV; *O*).

Somatic Inactivation of PDAC Tumor Suppressor Genes. Because our genetic data implicated germ-line lesions in *p16*^{Ink4a}, *p19*^{Arf}, and *p53* in promoting PDAC progression, we determined the presence of somatic alterations in these genes in primary tumors and early passage tumor cell cultures. In the *p53*$^{lox/lox}$ colony, elimination of p53 sequences was verified in all samples analyzed, and 10 of 10 tumors showed robust p19^{Arf} expression and WT *p19*^{Arf} coding sequences (Fig. 2 *A* and *B* and data not shown). Examination of p16^{Ink4a} status showed that four of four *p53*$^{lox/lox}$ *p16*$^{Ink4a+/+}$ tumor cell lines retained p16^{Ink4a} expression, whereas two of four *p53*$^{lox/lox}$ *p16*$^{Ink4a+/-}$ tumors showed markedly reduced or absent p16^{Ink4a} expression (Fig. 2*B* and data not shown). These observations, coupled with retention of p53 in all PDAC specimens from *p16*^{Ink4a}/*p19*$^{Arf\ lox/lox}$ mice (24), suggest that p53 and p19^{Arf} serve critical yet largely redundant roles in constraining PDAC progression in the mouse and indicate that *p16*^{Ink4a} loss is not required for PDAC progression in the context of early p53 inactivation. As noted above, however, a cooperative tumorigenic effect of *p53* and *p16*^{Ink4a} lesions was observed in the *p53*$^{lox/+}$ *p16*$^{Ink4a+/-}$ model. Analysis of derivative tumor cultures from these animals revealed loss of the WT *p53* allele in six of six cases (Fig. 2*C* and data not shown) and low/absent p16^{Ink4a} expression in five of six cases (Fig. 2*D*, lanes 1–6). In contrast, all tumor cell lines expressed p19^{Arf} at comparable levels to the *p53*$^{lox/lox}$ model (Fig. 2*D*). Consistent with the reduced/absent p16^{Ink4a} expression, there was deletion of WT *p16*^{Ink4a} sequences in one of six tumor cultures (Fig. 2*E*, lane 5) and hypermethylation of the *p16*^{Ink4a} promoter in three of six cases, as determined by methylation-specific PCR (Fig. 2*F*, lanes 1, 4, and 5). Similar findings were obtained in a larger group of tumors that were not exposed to cell culture (see the supporting information, which is published on the PNAS web site).

Comparable molecular analysis was performed in the *p16*^{Ink4a}/*p19*$^{Arf\ lox/+}$ model. As expected, low-passage p16^{Ink4a}/p19$^{Arf\ lox/+}$ tumor cultures uniformly lacked p16^{Ink4a} and p19^{Arf} protein expression (Fig. 3*A*; $n = 8$), and seven of eight samples sustained loss of the WT *p16*^{Ink4a}/*p19*^{Arf} allele (Fig. 3*B*). p53 showed low baseline expression, whereas γ-IR led to increased p53 protein levels and Ser-15 phosphorylation consistent with a physically intact p53 allele (Fig. 3*C*). Additional molecular analysis was performed on two PDACs arising after 1 year in *Pdx1-Cre LSL-Kras*^{G12D} animals without predisposing tumor suppressor mutations. Early passage tumor cultures and primary tumor lysates showed lack of both p16^{Ink4a} and p19^{Arf} expression by Western blot analysis (Fig. 3*D* and data not shown). Furthermore, extinction of expression was associated with homozygous loss of the *p16*^{Ink4a}/*p19*^{Arf} locus as detected by PCR analysis (Fig. 4*E*). Taken together, our results are in keeping with a model of PDAC tumor suppression in which specific barriers to Kras^{G12D}-directed tumorigenesis are provided by the p19^{Arf}-p53 and p16^{Ink4} pathways.

Genomic Aberrations in Mouse Models of PDAC. The availability of classes of tumors that either retained or lost expression of p53, p16^{Ink4a}, and p19^{Arf} enabled an assessment the impact of these lesions on the level of genomic instability and on the acquisition of specific regional gains or losses of chromosomes. To investigate the possible existence of clonal cooperating genetic lesions, we performed array-comparative genomic hybridization (aCGH) using a high-resolution oligonucleotide microarray on early passage PDAC cells lines from the *p16*^{Ink4a}/*p19*$^{Arf\ lox/lox}$ ($n = 16$), *p16*^{Ink4a}/*p19*$^{Arf\ lox/+}$ ($n = 8$), *p53*$^{lox/+}$ *p16*$^{Ink4a+/-}$ ($n = 6$), and *p53*$^{lox/lox}$ ($n = 10$) models. Intergenotype comparisons of overall genomic instability revealed subtle differences among the various PDAC models, with p53 mutant tumors trending toward an increased genomic complexity (see the supporting information). It is notable that analysis of eight human PCAC cell lines using the same aCGH platform revealed significantly higher numbers of chromosomal copy number alterations (CNAs) compared with the mouse tumors ($P < 0.001$; see the supporting information).

The aCGH analyses revealed distinct classes of profiles between the mouse genotypes. Hierarchical clustering of the aCGH profiles by using the Pearson correlation as a distance metric yielded three distinct clusters that largely segregated according to *p16*^{Ink4a}/*p19*^{Arf} or *p53* status (Fig. 4*A*). *p16*^{Ink4a}/*p19*^{Arf}-deficient tumors mainly fell into two clusters (6/8 tumors in cluster 1 and 13/14 tumors in cluster 2), whereas *p53*-deficient specimens predominated in the final cluster (13/16 tumors in cluster 3). A notable feature of cluster 2 was copy number increases in chromosome 6 containing the *Kras* locus. Although gains of the entire chromosome were noted, in a number of cases, the alterations were highly focal, spanning <1 Mb, indicating that *Kras* was the target of this event (Fig. 4*B*). Amplification of chromosome 6 occurred with much greater frequency in *p16*^{Ink4a}/*p19*^{Arf} mutant tumors (75%) than in *p53* mutant tumors (31%) (Table 2). Recurrent and genotype-specific alterations also occurred in the form of focal gains in chromosome 15 spanning the *c-Myc* locus (Fig. 4 *C* and Table 2; 31% of p53 mutant tumors vs.

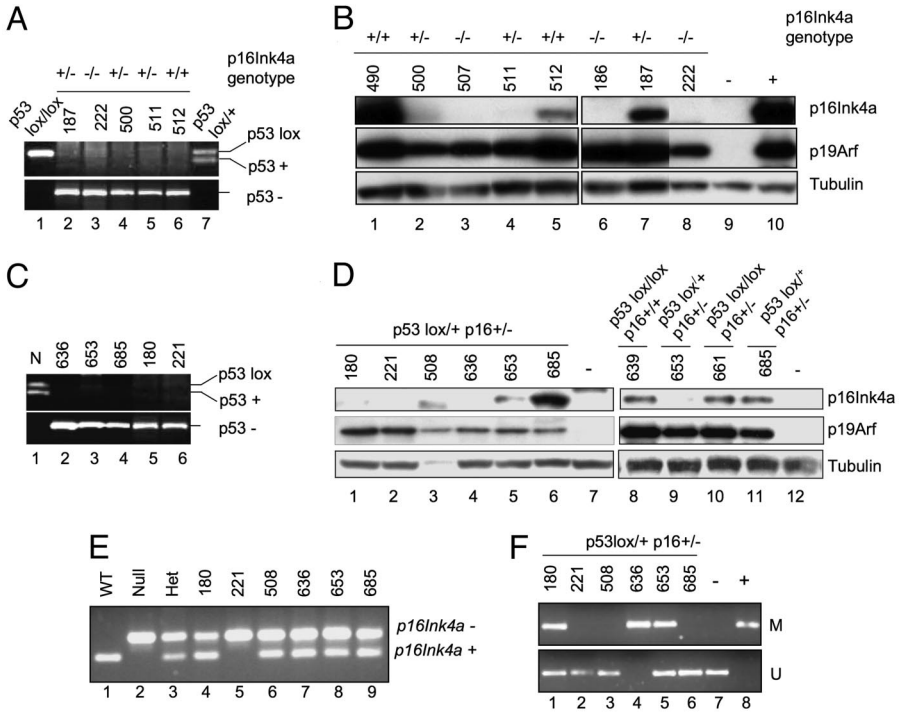

Fig. 2. Molecular analyses of PDAC cell lines and primary tumor specimens from mice with p53 and p16 mutant animals. (*A*) PCR reactions to detect the *p53*-WT (+) and $p53^{lox}$ alleles (*Upper*) and *p53*-null (−) allele (*Lower*) in normal tissue from $p53^{lox/lox}$ (lane 1) and $p53^{lox/+}$ (lane 7) mice and tumor cell lines (lanes 2–6). All tumor cell lines show only the *p53*-null allele. Germ-line $p16^{Ink4a}$ status is indicated at the top. (*B*) Western blot for $p16^{Ink4a}$ and $p19^{Arf}$ expression in cell lines derived from $p53^{lox/lox}$ mice with various $p16^{Ink4a}$ genotypes. The negative and positive controls are in lanes 9 and 10, respectively. α-Tubulin is shown as a loading control. (*C*) PCR analysis of the $p53^{+}$ and $p53^{lox}$ alleles (*Upper*) and the $p53^{-}$ (/) allele (*Lower*) demonstrates loss of the $p53^{+}$ allele in all tumors from $p53^{lox/+}$ $p16^{+/-}$ mice (lanes 2–6). Lane 1 shows the WT control specimen. (*D*) Western blot analysis shows low or absent $p16^{Ink4a}$ expression in five of six tumor cell lines from $p53^{lox/+}$ $p16^{+/-}$ mice (*Right*, lanes 1–6), whereas all retain $p19^{Arf}$ expression. Negative controls are in lanes 7 and 12. $p16^{Ink4a}$ expression in PDAC cell lines from $p53^{lox/lox}$ $p16^{+/+}$ (lane 8) and $p53^{lox/lox}$ $p16^{+/-}$ (lane 10) mice is shown as a reference (*Right*). (*E*) PCR analysis of the $p16^{Ink4a-}$ and $p16^{Ink4a+}$ alleles demonstrates LOH in one of six samples (lane 5). Normal tissue specimens are shown as controls for the $p16^{Ink4a+/+}$, $p16^{Ink4a-/-}$, and $p16^{Ink4a+/+}$ alleles (lanes 1–3). (*F*) Methylation-specific PCR assay to detect methylated CpG islands in the $p16^{Ink4a}$ promoter region reveals hypermethylation in three tumor lines (lanes 1, 4, and 5). *Upper* and *Lower* show the methylated (M) and unmethylated (U) alleles, respectively. Negative and positive controls are in lanes 7 and 8.

8% of the $p16^{Ink4a}/p19^{Arf}$ mutant tumors) and deletion of chromosome 4 in the vicinity of the $p16^{Ink4a}/p19^{Arf}$ locus (Fig. 4*A*; 50% of tumors from $p16^{Ink4a}/p19^{Arf\,lox/+}$ mice and one of six tumors from $p53^{lox/+}$ $p16^{Ink4a+/-}$ mice). These genomic distinctions within the data set were validated by using an alternative unsupervised clustering approach (D. Carrasco, unpublished work; see supporting information). These approaches demonstrate that CNA patterns including amplifications of *Kras* and *c-Myc* effectively identify classes of tumors that reflect the underlying tumor suppressor genotype. Other CNAs were also documented in these mouse PDAC genomes, including recurrent gains on chromosomes 1q, 4q, 8q, 16q, 17q, and 18q as well as losses on chromosomes 9q, 10q, 14q, and 17q (Fig. 4*A* and supporting information). Importantly, several focal and recurrent CNAs, such as 16q amplification and 17q deletion, are syntenic to recurrent CNAs in sporadic human PDAC (32, 33). Thus, these CNAs provide both a measure of molecular validation of murine PDAC models and a potential means of facilitating identification of PDAC progression genes.

Discussion

Both $p16^{Ink4a}$ and Arf-p53 Are Barriers to Mouse PDAC Progression. This study provides several lines of evidence establishing that both components of the $p16^{Ink4a}/p19^{Arf}$ locus provide critical barriers to

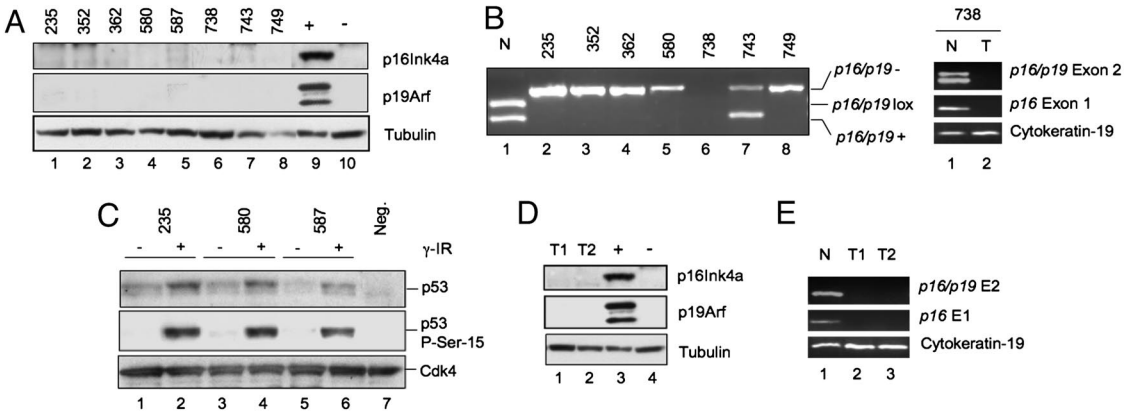

Fig. 3. Molecular analyses of PDAC cell lines from $p16^{Ink4a}/p19^{Arf\,lox/+}$ and $p16^{Ink4a}/p19^{Arf+/+}$ mice. (*A*) Western blot analysis $p16^{Ink4a}$ and $p19^{Arf}$ expression in lysates from tumor cell lines from $p16^{Ink4a}/p19^{Arf\,lox/+}$ mice. (*B*) PCR analysis of $p16^{Ink4a}/p19^{Arf}$ alleles in tumor cell lines from $p16^{Ink4a}/p19^{Arf\,lox/+}$ mice shows only the recombined $p16^{Ink4a}/p19^{Arf}$ allele (*Left*, lanes 2–8). Normal tissue from $p16^{Ink4a}/p19^{Arf\,lox/+}$ mice shows WT (+) and unrecombined (lox) alleles. Tumor no. 738 (*Left*, lane 6; *Right*, lane 2) shows a biallelic deletion of the entire $p16^{Ink4a}/p19^{Arf}$ locus. (*C*) Western blot analyses of γ-irradiated tumor cell lines (+) shows induction of total p53 protein levels and phosphorylation of p53 on Ser-15, consistent with present and functional p53 protein. −, untreated. Cdk4 protein levels are shown as a loading control. (*D*) Western blot analysis shows absence of $p16^{Ink4a}$ and $p19^{Arf}$ expression in *Pdx1-Cre LSL-*$Kras^{G12D}$ cell lines (lanes 1 and 2). Lanes 3 and 4 show positive and negative controls. (*E*) PCR analysis for the presence of $p16^{Ink4a}/p19^{Arf}$ exon 2, $p16^{Ink4a}$ exon 1, and *cytokeratin 19* sequences in cell lines from *Pdx1-Cre LSL-*$Kras^{G12D}$ mice (lanes 2 and 3) demonstrates biallelic deletion of $p16^{Ink4a}/p19^{Arf}$. Lane 1 shows normal control DNA.

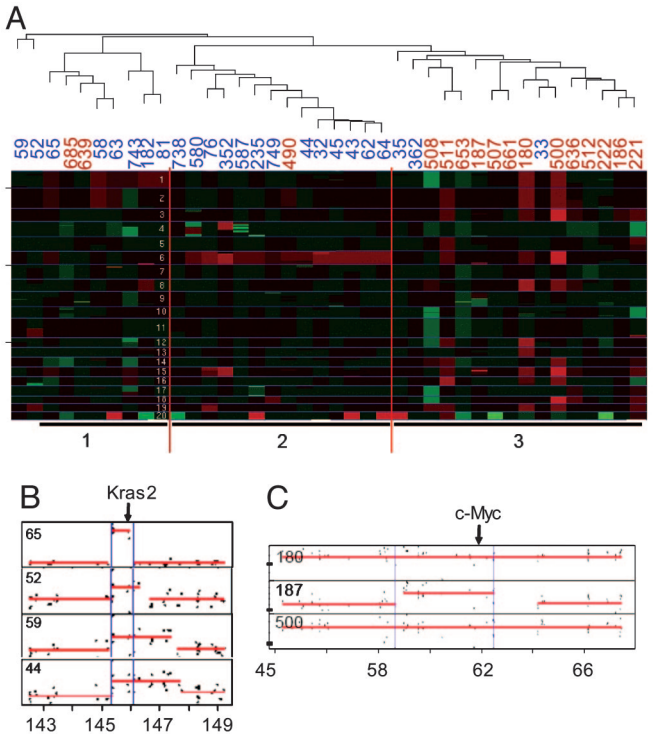

Fig. 4. aCGH analysis of mouse PDAC. (*A*) Hierarchical clustering of aCGH profiles reveals three distinct clusters. Sample names are given above the profile followed by an underscore and the genotype class (i.e., ''106_6'' indicates the profile for tumor no. 106, which is in genotype class 6. The genotype classes are: 1, $p53^{lox/lox}$;$p16^{Ink4a\ +/+}$; 2, $p53^{lox/lox}$;$p16^{Ink4a\ +/-}$; 3, $p53^{lox/lox}$;$p16^{Ink4a\ -/-}$; 4, $p53^{lox/+}$;$p16^{Ink4a\ +/-}$; 5, $p16^{Ink4a}$/$p19^{Arf\ lox/+}$; 6, $p16^{Ink4a}$/$p19^{Arf\ lox/lox}$. (*B* and *C*) Focal amplifications of *Kras2* in $p16^{Ink4a}$/$p19^{Arf}$-deficient (*B*) and *Myc* in *p53*-deficient (*C*) tumors are shown. Minimal common regions of amplification are shown by blue lines.

PDAC progression. Specifically, mice with homozygous mutations in either *p53* or $p16^{Ink4a}$ developed tumors with short latency; moreover, mice with combined heterozygous mutations in *p53* and $p16^{Ink4a}$ developed PDAC that predominantly lost expression of products of both genes but showed robust expression of $p19^{Arf}$. Tumors arising in $p16^{Ink4a}/p19^{Arf\ lox/+}$ animals lost both products of this locus but retained p53. Two aspects of this analysis are notable. First, although sharp distinctions have been drawn between Arf and p53 function in several other models and p53 has Arf-independent activities and vice versa (12), our PDAC models demonstrate that the roles of these tumor suppressors overlap significantly with regard to PDAC progression in the mouse. A second observation relates to the role of $p16^{Ink4a}$ loss in the setting of p53 inactivation. Specifically, whereas heterozygous deletion of *p53* and $p16^{Ink4a}$ during Kras initiation begets subsequent inactivation of the WT alleles of both genes during PDAC progression, loss of p53 function in the context of intact $p16^{Ink4}$ is not associated with subsequent $p16^{Ink4a}$ loss (this study and ref. 25). Possible explanations for this discrepancy include: (*i*) early and/or uniform homozygous loss of p53 coincident with Kras activation enables bypass of $p16^{Ink4a}$-mediated RB pathway tumor suppressor functions that would otherwise be operative; or (*ii*) there are species-specific differences in the tumor suppressor functions between human and mouse $p16^{Ink4a}$ and p53, as suggested by other studies (26). Irrespective, the double-heterozygous models reflect well the human situation in regard to the complimentary benefits of their concomitant loss and, thus, will provide a highly appropriate model system for studying aspects of PDAC progression.

Table 2. Gain/amplification of *Kras2* and *Myc* in mouse PDAC

Genotype	Kras2, %	Myc, %
$p53^{lox/lox}$ (n = 10)	40	30
$p53^{lox/+}$ (n = 6)	17	33
All p53 (n = 16)	31	31
$p16^{Ink4a}/p19^{Arf\ lox/lox}$ (n = 16)	81	6
$p16^{Ink4a}/p19^{Arf\ lox/+}$ (n = 8)	63	13
All $p16^{Ink4a}/p19^{Arf}$ (n = 24)	75	8

Tumor Suppressor Gene Status Influences Tumor Biology. Different combinations of tumor suppressor gene mutations, in conjunction with $Kras^{G12D}$ expression, all promoted the progression of PanIN to PDAC but produced tumors with varying spectra of clinical and histological features. Although tumors in all genotypes showed extensive local invasion and micrometastases, gross metastases were only prominent in mice with engineered heterozygous tumor suppressor deletions ($p16^{Ink4a}/p19^{Arf\ lox/+}$ or $p53^{lox/+}$ $p16^{Ink4a\ lox/+}$ mice) but not in mice with engineered homozygous deletions. Because the homozygous animals rapidly developed a lethal tumor burden, often with multiple primary tumors, these results raise the possibility that factors relating to tumor latency rather than the specific $p16^{Ink4a}$-RB or $p19^{Arf}$-p53 pathway lesions are primarily responsible for modulating metastatic behavior.

With respect the effect of genotype on tumor histology, the p53-deficient cohorts showed the higher prevalence of well differentiated ductal adenocarcinoma compared with the $p16^{Ink4a}/p19^{Arf}$-deficient animals (Table 1). Conversely, undifferentiated sarcomatoid histology was significantly reduced in p53-deficient models. These results are consistent with observations that $Kras^{G12D}$ and $p53^{R172H}$ alleles produce primarily ductal adenocarcinomas (25). Anaplastic carcinoma, although common in the homozygous models, was never the principal histological component in the heterozygous $p53^{lox/+}$ $p16^{Ink4a+/-}$ tumors and was completely absent in the $p16^{Ink4a}/p19^{Arf\ lox/+}$ model. In humans, ductal adenocarcinoma histology predominates, and the sarcomatoid and anaplastic subtypes are considered uncommon variants of PDAC with more aggressive clinical behavior, although they all appear to have comparable spectra of genetic lesions (34, 35). Our mouse models collectively recapitulate these different histologic variants, albeit at different frequencies than seen in spontaneous human tumors. Overall, these observations suggest that the set of tumor suppressor lesions strongly influences the cell differentiation phenotypes of the resulting tumors.

Recurrent Genomic Aberrations Arise During PDAC Progression. Genomic analysis revealed an effect of tumor suppressor genotype on the profile of tumor-associated chromosomal alterations and only modest trends toward increased genomic instability in p53 mutant tumors on the basis of the number of CNAs per tumor. Notably, the degree of genomic instability occurring in each of these PDAC mouse models is significantly less than that observed in human specimens (this study and refs. 32 and 33). This may reflect a bias imposed through the use of genetically engineered mouse models (i.e., p53 loss and KRAS activation may obviate the need for many further cytogenetic aberrations) or cross-species differences in chromosome biology and structure, particularly telomeres (5, 36, 37). The patterns of regional alterations in chromosomal copy number differed between tumors of different genotypes, suggesting that chromosomal alterations may harbor genes in which altered expression may specifically cooperate with distinct tumor suppressor gene mutations. Notable copy number gains at chromosome 6 encompassing the *Kras* locus were more commonly observed in the $p16^{Ink4a}/p19^{Arf}$ mutant tumors. This correlation may reflect the capacity of Kras to activate both the $p16^{Ink4a}$ and $p19^{Arf}$ promoters leading to cellular senescence *in vivo* (8, 38). $p16^{Ink4a}/p19^{Arf}$-deficient tumors may be especially permissive for

$Kras^{G12D}$ amplification, facilitating the cellular transformation associated with increased Kras signaling. In contrast, chromosome 15 gains overlapping the *Myc* locus were much more common in the *p53* mutant tumors. The selective amplification of *Myc* in association with p53 mutation has been noted in genomic analysis of melanomas harboring either p53 or $p16^{Ink4a}/p19^{Arf}$ mutations (39). In these contexts, Myc amplification may serve to bypass the inhibition of CDK4 activity and consequent cell-cycle arrest conferred by elevated $p16^{Ink4a}$ expression (39, 40). It is notable that, in the subset of $p53^{lox/lox}$ and $p53^{lox/+}$ tumors retaining robust $p16^{Ink4a}$ expression, other RB pathway components remained intact as evidenced by the absence of $p16^{Ink4a}$ and *Cdk4* mutations in full-length sequence analyses and the lack of perturbations in expression of RB and cyclin D1 (data not shown).

Amplifications of *KRAS* on chromosome 12q12 and *MYC* at 8q24 as well as deletions of $p16^{INK4A}$ on 9p21 are commonly observed in human pancreatic adenocarcinoma (32, 33). In addition to CNAs harboring validated pancreatic cancer genes, we have also identified additional mouse CNAs that are syntenic to human PDAC loci (see supporting information). Recurrence of these loci in multiple different tumor specimens and their evolutionary conservation indicate that they may harbor cancer genes with prime importance in PDAC pathogenesis. Moreover, the targeting of syntenic loci in these mouse PDACs highlights the potential of mouse models of cancer to serve as effective filters in the identification of cancer genes present in complex human copy number data sets.

Materials and Methods

Mouse Strains, Histopathology, and Establishment of Primary PDAC Cell Lines. The mouse strains in this study included the following alleles: $LSL\text{-}Kras^{G12D}$ (41), *Pdx1-Cre* (27), conditional $p53^{lox}$ (30), conditional $p16^{Ink4a}/p19^{Arf\,lox}$ (24), and a germ-line $p16^{Ink4a}$-specific null allele (that retains WT $p19^{Arf}$) (29). All experiments were performed on >87.5% FVB/n background. Some mice with the $p16^{Ink4a}/p19^{Arf\,lox}$ allele developed lymphomas (latency 28–60 weeks) that occurred independently of concurrent expression of *Pdx1-Cre* or $LSL\text{-}Kras^{G12D}$. The $p16^{Ink4a}/p19^{Arf\,lox}$ allele shows intact expression and function of the $p16^{Ink4a}/p19^{Arf}$ locus in cell culture-based assays *in vitro*, and it appears that the lymphomas arising in these mice are attributable to hypomorphic activity of $p16^{Ink4a}/p19^{Arf\,lox}$ allele. In addition, a subset of mice from both the $p16^{Ink4a}/p19^{Arf\,lox/+}$ and $p53^{lox/+}$ $p16^{Ink4a+/-}$ colonies developed progressive wasting in the absence of evident neoplastic growth, whereas some others developed cutaneous papillomas. These phenotypes are likely due to the extrapancreatic expression of $Kras^{G12D}$ induced by the *Pdx1-Cre* transgene because they are not observed in the context of the *p48-Cre* strain in which expression pattern is more tightly restricted to the pancreas (data not shown). Tissue processing, immunohistochemical staining, and establishment of primary PDAC cell lines were performed as described in ref. 24. The histological classification of each tumor reported in Table 1 was determined by evaluation of cross-sectional slides from two axes. The histological type representing the largest cross-sectional area was considered the primary component.

Molecular Analysis. RNA and DNA isolation, protein extract preparation from PDAC cell lines, and primary tumors was performed as described in ref. 24. For loss of heterozygosity analysis of $p16^{Ink4a}$, *p53*, and $p16^{Ink4a}/p19^{Arf}$, DNA was extracted from the early passage cell lines and amplified by PCR. Methylation-specific PCR analysis was performed as described in ref. 42.

Genomic Analysis. aCGH and data analysis was performed as described on Agilent mouse development or human 1A oligonucleotide microarrays (see supporting information) (32).

We thank David Tuveson and Tyler Jacks for the $LSL\text{-}Kras^{G12D}$ mice; Anton Berns for the $p53^{lox}$ mice; Doug Melton for the *Pdx1-Cre* mice; and Alice Yu, Karen Marmon, and Shan Jiang for expert monitoring of the mouse colony. T. R. Devereux generously provided the Sp6c lung cancer cell line. This work was supported by grants from the National Institutes of Health (to R.A.D. and N.B.). R.A.D. is an American Cancer Society Research Professor.

1. Parkin, D. M., Bray, F., Ferlay, J. & Pisani, P. (2005) *CA Cancer J. Clin.* **55,** 74–108.
2. Jemal, A., Murray, T., Ward, E., Samuels, A., Tiwari, R. C., Ghafoor, A., Feuer, E. J. & Thun, M. J. (2005) *CA Cancer J. Clin.* **55,** 10–30.
3. Hruban, R. H., Wilentz, R. E. & Kern, S. E. (2000) *Am. J. Pathol.* **156,** 1821–1825.
4. DiGiuseppe, J. A., Hruban, R. H., Offerhaus, G. J., Clement, M. J., van den Berg, F. M., Cameron, J. L. & van Mansfeld, A. D. (1994) *Am. J. Pathol.* **144,** 889–895.
5. van Heek, N. T., Meeker, A. K., Kern, S. E., Yeo, C. J., Lillemoe, K. D., Cameron, J. L., Offerhaus, G. J., Hicks, J. L., Wilentz, R. E., Goggins, M. G., *et al.* (2002) *Am. J. Pathol.* **161,** 1541–1547.
6. Rozenblum, E., Schutte, M., Goggins, M., Hahn, S. A., Panzer, S., Zahurak, M., Goodman, S. N., Sohn, T. A., Hruban, R. H., Yeo, C. J. & Kern, S. E. (1997) *Cancer Res.* **57,** 1731–1734.
7. Sharpless, N. E. (2005) *Mutat. Res.* **576,** 22–38.
8. Serrano, M., Lin, A. W., McCurrach, M. E., Beach, D. & Lowe, S. W. (1997) *Cell* **88,** 593–602.
9. Michaloglou, C., Vredeveld, L. C., Soengas, M. S., Denoyelle, C., Kuilman, T., van der Horst, C. M., Majoor, D. M., Shay, J. W., Mooi, W. J. & Peeper, D. S. (2005) *Nature* **436,** 720–724.
10. Pomerantz, J., Schreiber-Agus, N., Liegeois, N. J., Silverman, A., Alland, L., Chin, L., Potes, J., Chen, K., Orlow, I., Lee, H. W., *et al.* (1998) *Cell* **92,** 713–723.
11. Zhang, Y., Xiong, Y. & Yarbrough, W. G. (1998) *Cell* **92,** 725–734.
12. Lowe, S. W. & Sherr, C. J. (2003) *Curr. Opin. Genet. Dev.* **13,** 77–83.
13. Sugimoto, M., Kuo, M. L., Roussel, M. F. & Sherr, C. J. (2003) *Mol. Cell* **11,** 415–424.
14. Itahana, K., Bhat, K. P., Jin, A., Itahana, Y., Hawke, D., Kobayashi, R. & Zhang, Y. (2003) *Mol. Cell* **12,** 1151–1164.
15. Schutte, M., Hruban, R. H., Geradts, J., Maynard, R., Hilgers, W., Rabindran, S. K., Moskaluk, C. A., Hahn, S. A., Schwarte-Waldhoff, I., Schmiegel, W., *et al.* (1997) *Cancer Res.* **57,** 3126–3130.
16. Whelan, A. J., Bartsch, D. & Goodfellow, P. J. (1995) *N. Engl. J. Med.* **333,** 975–977.
17. Goldstein, A. M., Fraser, M. C., Struewing, J. P., Hussussian, C. J., Ranade, K., Zametkin, D. P., Fontaine, L. S., Organic, S. M., Dracopoli, N. C., Clark, W. H., Jr., *et al.* (1995) *N. Engl. J. Med.* **333,** 970–974.
18. Hustinx, S. R., Leoni, L. M., Yeo, C. J., Brown, P. N., Goggins, M., Kern, S. E., Hruban, R. H. & Maitra, A. (2005) *Mod. Pathol.* **18,** 959–963.
19. Vousden, K. H. & Lu, X. (2002) *Nat. Rev. Cancer* **2,** 594–604.
20. Maitra, A., Adsay, N. V., Argani, P., Iacobuzio-Donahue, C., De Marzo, A., Cameron, J. L., Yeo, C. J. & Hruban, R. H. (2003) *Mod. Pathol.* **16,** 902–912.
21. Boschman, C. R., Stryker, S., Reddy, J. K. & Rao, M. S. (1994) *Am. J. Pathol.* **145,** 1291–1295.
22. Heinmoller, E., Dietmaier, W., Zirngibl, H., Heinmoller, P., Scaringe, W., Jauch, K. W., Hofstadter, F. & Ruschoff, J. (2000) *Am. J. Pathol.* **157,** 83–92.
23. Hingorani, S. R., Petricoin, E. F., Maitra, A., Rajapakse, V., King, C., Jacobetz, M. A., Ross, S., Conrads, T. P., Veenstra, T. D., Hitt, B. A., *et al.* (2003) *Cancer Cells* **4,** 437–450.
24. Aguirre, A. J., Bardeesy, N., Sinha, M., Lopez, L., Tuveson, D. A., Horner, J., Redston, M. S. & DePinho, R. A. (2003) *Genes Dev.* **17,** 3112–3126.
25. Hingorani, S. R., Wang, L., Multani, A. S., Combs, C., Deramaudt, T. B., Hruban, R. H., Rustgi, A. K., Chang, S. & Tuveson, D. A. (2005) *Cancer Cells* **7,** 469–483.
26. Rangarajan, A., Hong, S. J., Gifford, A. & Weinberg, R. A. (2004) *Cancer Cells* **6,** 171–183.
27. Gu, G., Dubauskaite, J. & Melton, D. A. (2002) *Development (Cambridge, U.K.)* **129,** 2447–2457.
28. Tuveson, D. A., Shaw, A. T., Willis, N. A., Silver, D. P., Jackson, E. L., Chang, S., Mercer, K. L., Grochow, R., Hock, H., Crowley, D., *et al.* (2004) *Cancer Cells* **5,** 375–387.
29. Sharpless, N. E., Bardeesy, N., Lee, K. H., Carrasco, D., Castrillon, D. H., Aguirre, A. J., Wu, E. A., Horner, J. W. & DePinho, R. A. (2001) *Nature* **413,** 86–91.
30. Marino, S., Vooijs, M., van Der Gulden, H., Jonkers, J. & Berns, A. (2000) *Genes Dev.* **14,** 994–1004.
31. Solcia, E., Capella, C. & Kloppel, G. (1995) *Tumors of the Pancreas* (Armed Forces Institute for Pathology, Washington, DC).
32. Aguirre, A. J., Brennan, C., Bailey, G., Sinha, R., Feng, B., Leo, C., Zhang, Y., Zhang, J., Gans, J. D., Bardeesy, N., *et al.* (2004) *Proc. Natl. Acad. Sci. USA* **101,** 9067–9072.
33. Heidenblad, M., Schoenmakers, E. F., Jonson, T., Gorunova, L., Veltman, J. A., van Kessel, A. G. & Hoglund, M. (2004) *Cancer Res.* **64,** 3052–3059.
34. Hoorens, A., Prenzel, K., Lemoine, N. R. & Kloppel, G. (1998) *J. Pathol.* **185,** 53–60.
35. Deckard-Janatpour, K., Kragel, S., Teplitz, R. L., Min, B. H., Gumerlock, P. H., Frey, C. F. & Ruebner, B. H. (1998) *Arch. Pathol. Lab. Med.* **122,** 266–272.
36. Maser, R. S. & DePinho, R. A. (2002) *Science* **297,** 565–569.
37. Blasco, M. A. (2005) *EMBO J.* **24,** 1095–1103.
38. Palmero, I., Pantoja, C. & Serrano, M. (1998) *Nature* **395,** 125–126.
39. Bardeesy, N., Bastian, B. C., Hezel, A., Pinkel, D., DePinho, R. A. & Chin, L. (2001) *Mol. Cell. Biol.* **21,** 2144–2153.
40. Alevizopoulos, K., Vlach, J., Hennecke, S. & Amati, B. (1997) *EMBO J.* **16,** 5322–5333.
41. Jackson, E. L., Willis, N., Mercer, K., Bronson, R. T., Crowley, D., Montoya, R., Jacks, T. & Tuveson, D. A. (2001) *Genes Dev.* **15,** 3243–3248.
42. Bardeesy, N., Morgan, J., Sinha, M., Signoretti, S., Srivastava, S., Loda, M., Merlino, G. & DePinho, R. A. (2002) *Mol. Cell. Biol.* **22,** 635–643.
43. Eisen, M. B., Spellman, P. T., Brown, P. O. & Botstein, D. (1998) *Proc. Natl. Acad. Sci. USA* **95,** 14863–14868.